Active compression bandage made of electroactive elastomers

Luigi Calabrese, Gabriele Frediani, Massimiliano Gei, Danilo De Rossi and Federico Carpi*

***Abstract*—Active compression bandages made of electro-mechanically active elastomers have recently been proposed to counteract dynamically, rather than statically, limb swelling due to various pathologies or conditions. To apply and modulate the compression pressure they exploit the ability of electroactive elastomer layer/s of changing size in response to a high voltage. For safety reasons such devices must be properly insulated from the user limb. In this work we present an electroactive bandage made of two pre-stretched layers of an electroactive acrylic elastomer sandwiched between two insulating layers of a passive silicone elastomer. Moreover, uniaxial stiffening elements where introduced to maximise actuation along the radial direction. Prototypes of the bandage were tested with a pressurized air chamber, which mimicked the compliance of a human limb. Both experimental investigations and a finite electro-elasticity analytical model showed that the passive layers play a key role for an effective transmission of actuation from the active layers to the load. The prototypes were able to actively vary the applied pressure up to 10%. The model showed that by increasing the number of electroactive layers the pressure variation could be further increased, although with a saturation trend, providing useful indication for future designs of such bandages.**

***Index Terms*— actuator, bandage, compressive, dielectric elastomer, electrical, electroactive, electromechanical, limb, polymer, soft, stretchable.**

I. Introduction

Blood circulation from the lower limbs to the heart depends on vein valves and muscular compression on blood vessels. When those mechanisms are pathological, blood tends to accumulate in the lower limbs [1]. This may cause swelling, pain or lead to even more severe conditions [2], [3]. Treatments for those diseases include both static (passive) and dynamic (active) compression systems, such as stockings and pneumatic sleeves [4], [5]. The former are elastic garments applying a static pressure, typically in the range 20-60 mmHg (2.7-8 kPa) [6], which however have been proved to be less effective than pneumatic systems [7], [8]. On the other hand, the latter require bulky pneumatic cuffs and a pumping box, resulting impractical in many conditions.

An alternative solution to address these issues comes from the use of Dielectric Elastomer (DE) actuators, which were proven to be effective for interacting with soft bodies [9]. In particular, their use for electro-mechanically active bandages was recently proposed [10], [11]. The device was conceived as a stretchable bandage consisting of a single layer of a silicone elastomer with compliant electrodes on both sides. The active bandage was designed to be wrapped around human limbs with an initial maximum pressure that can be dynamically reduced via an applied high-voltage. Considering the high voltage needed to activate the bandage, such device must prevent electrical discharges and guarantee proper insulation from both the human limb and the external environment.

To address this issue, in this work we present a dynamic active bandage featuring silicone elastomer coating layers, acting as insulators. Moreover, the coating layers are analysed also in terms of their effect on the transmission of actuation from the active layers to the load. Furthermore, this paper also presents the following means to improve the performance of such active bandages: a multi-layer structure for the active part, a more-performing active material and a design solution that maximises actuation along the radial direction.

Both experimental tests and a finite electro-elasticity model, specifically developed for the multilayer bandage, were used to investigate the effects on the actuation performance of the number of the active layers and the thickness of the coating passive layers.

II. Active Bandage Concept

The conceived active bandage relies on a particular type of Electromechanically Active Polymers (EAPs), which are smart materials able to respond to applied electrical stimuli with changes of size and/or shape [12], [13]. Specifically, we considered the most performing EAP technology, known as Dielectric Elastomer (DE) actuators [14]–[17].

DE actuators are electromechanical transducers essentially made of a thin layer of an insulating elastomer coated on both sides with compliant electrodes. When a voltage V is applied between the electrodes of a planar DE actuator, the following effective electrostatic pressure p, parallel to the electric field E, is generated [14]:

Asterisk indicates corresponding author.

*F. Carpi is with the Department of Industrial Engineering, University of Florence, Via di S. Marta, 3 - 50139 Florence, Italy (e-mail: federico.carpi@unifi.it; Phone: +39-055-2758660).

L. Calabrese is with the Department of Civil, Environmental and Mechanical Engineering, University of Trento, Trento, Italy (e-mail: luigi.calabrese@unitn.it) and with the Research Centre "E. Piaggio", University of Pisa, Largo L. Lazzarino, 2 – 56122 Pisa, Italy.

M. Gei is with the School of Engineering, Cardiff University, The Parade, Cardiff CF24 3AA, UK (e-mail: geim@cardiff.ac.uk).

G. Frediani is with the Department of Industrial Engineering, University of Florence, Via di S. Marta, 3 - 50139 Florence, Italy (e-mail: frediani.gabriele @gmail.com).

D. De Rossi is with the Information Engineering Department, University of Pisa, Pisa, Italy, and with the Research Centre "E. Piaggio", University of Pisa, Largo L. Lazzarino, 2 – 56122 Pisa, Italy (e-mail: d.derossi@centropiaggio.unipi.it).

$$p = \varepsilon_0 \varepsilon_r (V/d)^2 = \varepsilon_0 \varepsilon_r E^2, \quad (1)$$

where ε_0 is the dielectric permittivity of vacuum, ε_r is the relative dielectric constant of the elastomer and d is the thickness of the dielectric layer. This pressure squeezes the soft dielectric layer causing a reduction of its thickness and a concomitant expansion of its area [14].

The bandage was conceived as a thin, stretchable and electro-responsive multilayer structure of elastomer films, to be wrapped around limbs (Fig. 1). Two active layers (a_1 and a_2) are sandwiched between two passive layers (p_1 and p_2).

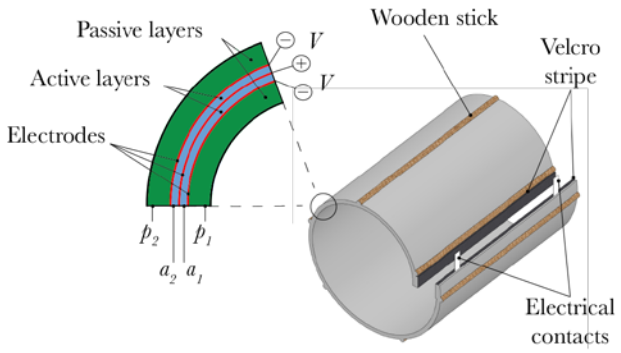

Fig. 1. Schematic representation of the proposed dynamic active bandage. The magnification shows the multilayer structure of the bandage, where two inner active layers (a_1 and a_2) are coupled to two passive layers (p_1 and p_2). Wooden stiffeners are embedded within the outer passive layer longitudinally in order to maximise actuation radially. Velcro stripes allow for securing the bandage to the limb.

Each inner active layer consists of a DE film coated with compliant electrodes. The two active layers are then coupled to thicker and softer passive layers. The passive layers have two key functions. Firstly, they serve as a mechanical interface with the limb, aimed at reducing the constraining effect introduced by the latter on the electrically induced deformation of the active layers. Secondly, as the proposed prototype bandage requires high driving voltages (as detailed in the following), the passive layers also ensure electrical safety, providing insulation.

Wooden stiffening sticks were embedded within the outer passive layer, with the aim of maximising actuation (variation of pressure) along the radial direction, preventing elongations of the bandage longitudinally. Indeed, combining a DE actuator with unstretchable elements has previously been demonstrated to be effective for unidirectional actuation [18].

The bandage was conceived to be wrapped around the limb with a certain prestretch, thus applying a certain passive pressure. When a voltage V is applied between the electrodes, the bandage is able to partially release the initial passive pressure, by increasing its circumference. Therefore, by modulating the applied voltage it is possible to continuously vary the applied pressure.

As mentioned above, prior to this work other investigators have reported on the use of DE actuators to develop active bandages [10], [11]. The peculiarities of the approach described here are: 1) two active layers were stacked together to increase the strength of the system; 2) the active layers were made of an acrylic elastomer film showing one of the highest electromechanical transduction performance, in terms of maximum achievable strains and stresses; 3) stiffening sticks were used to maximise actuation along the radial direction; 4) two thick and soft passive layers were used as interfaces with suitable properties in terms of mechanical compliance and electrical safety. The effects of these improvements were investigated theoretically and experimentally as reported in the following sections.

III. Active Bandage Specifications

The bandage should be able to apply a maximum pressure comparable to those of elastic compression stockings, i.e. 1-6 kPa [19], and then reduce the pressure upon electric driving. The literature does not offer any widely accepted exact estimate on the variation of pressure required to compensate for a deficient blood return. This is likely due to the variability of individual pathological and anatomical conditions. Indeed, for any given deficit, the compensation pressure could vary significantly according to the size of the limb, especially due to the thickness of muscles and adipose tissue. So, instead of targeting a specific performance, this work was aimed at validating the functionality of the proposed concept. This was achieved by manufacturing and characterising prototypes, as described below.

IV. Manufacturing of Prototype Active Bandages

Proof-of-concept prototype bandages were manufactured as follows. The active layers consisted of an acrylic elastomer film (VHB 4910, 3M, USA). This material was chosen in consideration of its well-known high electromechanical transduction performance in terms of achievable active stress [14], [15] and its adhesive properties, which simplified the manufacturing process by ensuring proper bonding between layers. The compliant electrode material consisted of carbon black powder (Vulcan XC72, Cabot Corporation, USA). The passive elastomeric layers were made of a soft silicone elastomer (TC-5005 A/B-C, BJB Enterprises Inc., USA), which was used with a content of softening agent C equal to 50 wt%. The passive elastomeric layers were produced by mould casting as films of different thickness, ranging from 2 to 4 mm. The different films were used to manufacture different samples of the bandage, in order to investigate how the electromechanical performance was affected by the thickness of the passive layers. Six wooden stiffening sticks, having a diameter of 2.5 mm each, were integrated within the outer passive layer, during its fabrication by mould casting, according to the layout shown in Fig. 2.

Electrical contacts for the electrodes were obtained by means of metal stripes integrated within the structure. Velcro stripes were glued at the two ends of the bandage, so as to secure it to the limb (Fig. 2).

The overall manufacturing process consisted of the following steps. A single active layer with a thickness at rest of 2 mm was obtained by coupling together two unstretched 1 mm-thick VHB 4910 films. This was justified by preliminary experimental evidences, which had shown superior force generation capabilities from actuators featuring thicker active layers. The resulting film was then equi-biaxially prestretched

by 300% and attached to a support frame. The use of that pre-strain was justified by its well-known beneficial effect in terms of electromechanical performance increase, as first reported by [14] and then explained in different ways by [16] and [20]. The prestretch caused a reduction of the thickness from 2 to 0.125 mm.

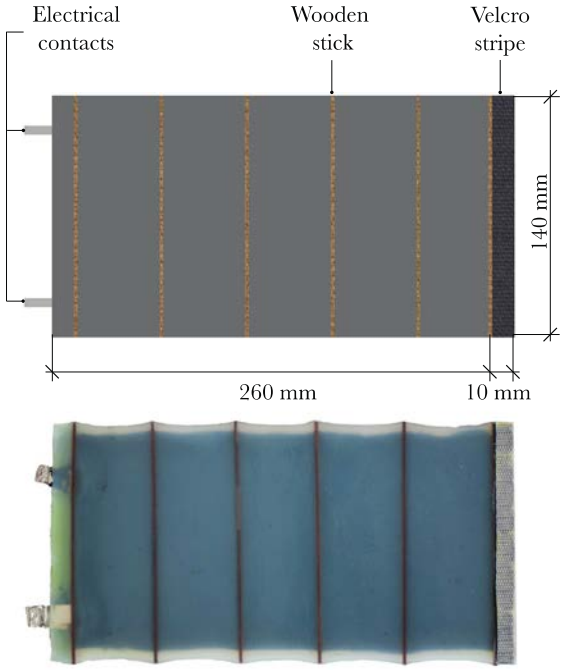

Fig. 2. Schematic drawing (top) and picture (bottom) of a prototype active bandage.

A first compliant electrode (250 mm × 120 mm) was then created by depositing an alcohol-based suspension of the carbon black powder on one of the surfaces of the active layer. Then, a metal stripe connector was attached to it. A second active layer was coupled to the first one, covering the electroded side. The outer surfaces of the two-layer structure were coated with the carbon black powder to obtain analogous compliant electrodes and were fitted with metal stripe connectors.

In order to create the passive layers, the active layer sandwich was laid at the bottom of a mould and then coated with the silicone material in liquid form, which was poured into the mould. The mould was maintained horizontally for curing at room temperature for 24 hours. After curing, the obtained multi-layer structure was removed from the mould and flipped over, and the same procedure was repeated in order to cast the second passive layer. During this process, six wooden sticks were also integrated on one side of the structure, by placing them on the surface of the active layer before the deposition of the silicone. The sticks allowed for holding the pre-stretch along one direction upon the removal of the bandage from the supporting frame.

The resulting self-standing bandage acquired the shape visible in Fig. 2. The extent of inevitable shrinking between two adjacent sticks depended on the passive layers thickness, according to the mechanical resistance offered by the passive coatings. Owing to that reason, it was not possible to obtain self-standing bandages with a passive layer thickness lower than 2 mm.

V. Testing of the Prototype Active Bandages

In order to test the performance of the different prototype bandages, a chamber that mimicked the compliance of a human limb was assembled. It consisted of a soft tubular structure containing pressurized air, as shown in Fig. 3a. It was constructed by coupling together two soft rubber membranes (model 4075 triaxial test rubber membrane, Wykeham Farrance, UK), having each a diameter of 70 mm and a thickness of 0.4 mm, and combining them with two rigid sealing plugs. The sealing plugs were connected one another by a rigid spacer, setting to 180 mm the distance between the two inner plugs edges. A manual pump, connected to one of the sealing plugs, allowed for pressurizing the air chamber. Pressure readings were taken from a digital pressure gauge (model Bit02B-2.5 bar, AEP Transducers, Italy), connected to the other sealing plug (Fig. 3).

Fig. 3. Testing of the prototype dynamic bandages: air chamber that mimicked the compliance of a human limb, without (a) and with (b) the bandage.

The bandage was secured (by means of the Velcro stripes) to the air chamber, such that the stiffening sticks were oriented axially (Fig. 3b). The chamber pressure was initially set to P_0=7.5 kPa for each prototype bandage tested. Therefore, the different bandages reached different initial values of their diameter, according to the different values of their passive layer thickness (and, so, their stiffness).

From this initial state, increasing voltages were applied, with steps of 500 *V*, until electrical breakdown of the bandage occurred. As a result of the radial actuation, the internal chamber pressure P_V reached a lower value, monitored with the pressure gauge. Results of the testing of three samples of the bandage with a passive layer thickness D_p of 2, 3 and 4 mm are presented in Fig. 4. The data show that 3 mm was an 'optimum' value, among those tested, for the passive layer thickness.

In order to obtain an analytical description of the system, an axisymmetric model of the bandage based on finite electro-elasticity was developed as described below.

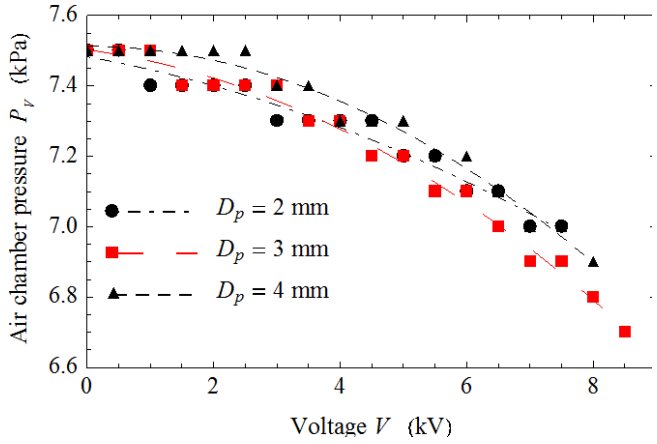

Fig. 4. Electromechanical performance of three samples of bandages having a different initial thickness D_p of their passive layers. Quadratic fitting curves are used as a guide for the eye.

VI. Analytical Model of the Active Bandage

The model neglected the viscoelastic behaviour of each layer and described its nonlinear electromechanical properties using a Neo-Hookean hyper-electro-elastic representation.

The model was developed for a central portion of the tubular structure, which was assumed to be sufficiently distant from the two ends of the tube to neglect any variation of pressure along the longitudinal coordinate *z*. Moreover, in consideration of the fact that the stiffening sticks constrain the longitudinal stretch to a fixed value, the length along the *z*-axis was considered constant (140 mm, see Fig. 2). Therefore, the problem was studied assuming a plane strain condition, implying a longitudinal stretch $\lambda_z = 1$ for the passive layers and $\lambda_z = 4$ for the active ones.

A. Kinematics of the multilayer structure

To describe the geometry of the system, the three deformed configurations reported in Fig. 5 were considered.

In the "initial state" $\mathcal{B}_b$ (Fig. 5 top), the bandage is wrapped around the air chamber with a circumferential length at the interface of 260 mm. Here, the system is in equilibrium with an air chamber pressure P_b and a contact pressure between the bandage and the chamber's rubber membrane P_{cb}. It is worth pointing out that when the bandage is applied to the chamber and the latter is pressurized, the azimuthal or hoop stress is distributed between the rubber membrane and the bandage, according to their stiffness. In this state $\mathcal{B}_b$, which is reached when the planar bandage is bent to reach the cylindrical configuration, the length of the inner circumference of the passive layer p_1 was assumed to be equal the length (260 mm) of the unbent bandage (Fig. 2). This way, the inner boundary of the layer p_1 has a hoop stretch $\lambda_{\theta b}$=1. In principle, it should be considered that, while bending the multilayer, a non-homogeneous deformation is imposed [21], which would induce a radius-dependent hoop stretch in the layers. However, due to the thinness of the strata, only the stretch of the midline of each layer $\lambda_{\theta b,\mathrm{lay}}$ (where 'lay' indicates the layer, namely lay=*m*, p_1, a_1, a_2, p_2) was considered in our model. A straightforward computation shows that for the active layers a_1, a_2 this hoop stretch ranges between 4.196 and 4.388 (as these layers are initially prestretched with a factor 4), while $\lambda_{\theta b,p1}$ ($\lambda_{\theta b,p2}$) ranges between 1.024 (1.075) and 1.046 (1.140). The stretch $\lambda_{\theta b,\mathrm{m}}$ is assumed unitary. Table 1 reports the calculated hoop stretches.

Table 1. Values of the hoop stretches of the midline in the initial configuration $\mathcal{B}_b$ for each layer of the three samples of bandages tested in state $\mathcal{B}_b$.

	D_p=2 mm	D_p=3 mm	D_p=4 mm
$\lambda_{\theta b,p1}$	1.024	1.035	1.046
$\lambda_{\theta b,a1}$	4.196	4.284	4.376
$\lambda_{\theta b,a2}$	4.208	4.296	4.388
$\lambda_{\theta b,p2}$	1.075	1.108	1.140

In the "Voltage OFF" state $\mathcal{B}_0$ (Fig. 5 centre), the bandage is secured to the air chamber with a certain circumferential stretch, assigned when the air chamber pressure $P_0 > P_b$ is set to 7.5 kPa. In this state, the contact pressure between the rubber membrane and the active bandage is $P_{c0} > P_{cb}$.

In the "Voltage ON" state $\mathcal{B}_V$ (Fig. 5 bottom), a voltage *V* generates a radial expansion of the bandage, which behaves like a cylindrical DE actuator [22], [23]. The radial expansion causes an active reduction of both the chamber's internal pressure and the contact pressure applied to the chamber, respectively from P_0 to $P_V < P_0$ and from P_{c0} to $P_c < P_{c0}$. In this state, the hoop stretch in the generic layer $\lambda_{\theta\mathrm{lay}}(r)$ is given by:

$$\lambda_{\theta\mathrm{lay}}(r) = \frac{r}{R}\lambda_{\theta b,\mathrm{lay}} = \frac{r}{\sqrt{R_{\mathrm{in,lay}}^2 + \lambda_z\left(r^2 - r_{\mathrm{lay}}^2\right)}}\lambda_{\theta b,\mathrm{lay}}\,, \qquad (2)$$

where lay=*m*, p_1, a_1, a_2, p_2 and $R_{in,\mathrm{lay}}$ denotes the inner radius of layer 'lay' in state $\mathcal{B}_b$. In (2), the ratio *r*/*R* is the hoop stretch with respect to $\mathcal{B}_b$, while $\lambda_{\theta b,\mathrm{lay}}$ takes into account the deformation undergone by the multilayer in state $\mathcal{B}_b$. The square root term is an alternative expression for the radius *R*, obtained by taking into account the constraint of incompressibility of the elastomeric material, i.e. $\lambda_r\lambda_z\lambda_\theta = 1$, which is useful to compute the radial stretch λ_r recalling that $\lambda_z = 1$.

B. Electro-mechanics of a single layer

In order to describe the overall behaviour of the multilayer, it is useful to recall the governing equations for a single layer in a cylindrical reference system.

Let us assume that the current inner and outer radii of an DE cylindrical actuator are r_i and r_e, respectively, and that at the two cylindrical surfaces the radial tensile stresses $\sigma_r(r_i)$ and $\sigma_r(r_e)$ are applied. In addition, the surfaces are coated with perfectly stretchable electrodes subjected to a voltage *V*, which induces through the thickness a radial electric field $E(r)=E_r(r)$.

An application of the Gauss' theorem at a generic radial distance within the dielectric provides a relation between *E* and the amount of charge *Q* stored on one electrode:

$$E = \frac{Q}{2\pi r \lambda_z L \varepsilon}, \tag{3}$$

where $\varepsilon = \varepsilon_0 \varepsilon_r$ is the absolute dielectric permittivity of the elastomer.

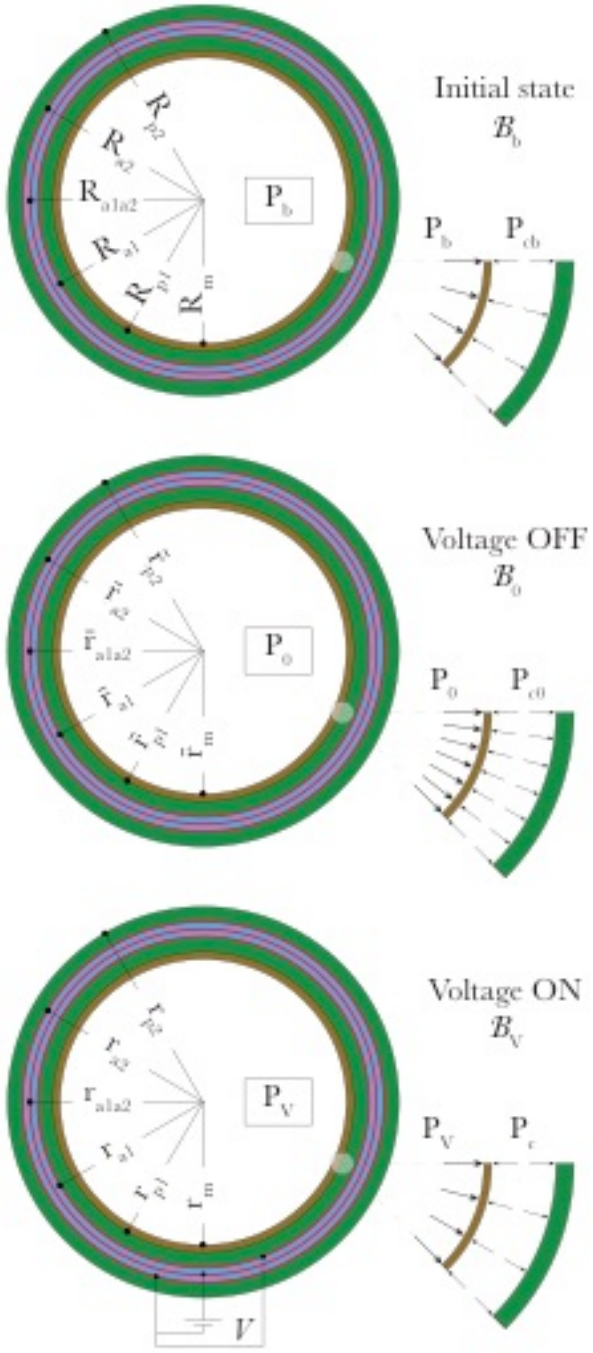

Fig. 5. Schematic representation of the cross-section of the air chamber surrounded by the active bandage. (a) In the "initial state" $\mathcal{B}_b$, the active bandage is secured around the rubber membrane of the chamber with an air chamber pressure P_b and a contact pressure P_{cb}, so that the bandage's inner radius R_{p1} is ≈ 40 mm (radial distances are denoted by the letter R), (b) In the "Voltage OFF" state $\mathcal{B}_0$, the air chamber pressure is manually set to P_0=7.5 kPa, causing an expansion of the bandage (radial distances are denoted by r). (c) Following the application of a voltage V, the system is switched to its "Voltage ON" state $\mathcal{B}_V$, where the air chamber pressure decreases from P_0 to a lower value P_V and the contact pressure drops from P_{c0} to $P_c < P_{c0}$ (radial distances are denoted by the letter r).

By integrating (3) with respect to the radius while considering the well-known relation between the electric potential φ and electric field E for a cylindrical capacitor having an axial length L, we obtain the relation between Q and the applied voltage V:

$$V = \varphi(r_i) - \varphi(r_e) = \int_{r_i}^{r_e} -d\varphi = \int_{r_i}^{r_e} E dr = \\ = \frac{Q}{2\pi\varepsilon\lambda_z L}\int_{r_i}^{r_e}\frac{1}{r}dr = \frac{Q}{2\pi\varepsilon\lambda_z L} ln\frac{r_e}{r_i}, \tag{4}$$

so that

$$E = \frac{1}{r}\, V / ln\frac{r_e}{r_i}. \tag{5}$$

The layer, incompressible, obeys an isotropic hyper-electro-elastic strain energy $W(\lambda_r, \lambda_\theta, \lambda_z, E)$. In this configuration, the constitutive equations can be written as (see Appendix):

$$D = -\frac{\partial W}{\partial E}, \tag{6}$$

$$\sigma_\theta - \sigma_r = \lambda_\theta \frac{\partial W}{\partial \lambda_\theta} - \lambda_r \frac{\partial W}{\partial \lambda_r} - DE, \tag{7}$$

$$\sigma_z - \sigma_r = \lambda_z \frac{\partial W}{\partial \lambda_z} - \lambda_r \frac{\partial W}{\partial \lambda_r} - DE, \tag{8}$$

where D is the electric displacement, which has only a radial component, according to (6).

Under the action of an axisymmetric electromechanical loading, the equilibrium of each layer is governed, in terms of Cauchy total stress $\boldsymbol{\sigma}$, by the following differential equation:

$$\frac{d\sigma_r}{dr} + \frac{\sigma_r - \sigma_\theta}{r} = 0. \tag{9}$$

Integration of (9) between r_i and r_e provides

$$\sigma_r(r_e) - \sigma_r(r_i) = \int_{r_i}^{r_e} \frac{\sigma_\theta - \sigma_r}{r} dr. \tag{10}$$

In our model, an extended neo-Hookean strain energy function was adopted to compare model predictions with experimental results. Its general expression is

$$W = \frac{1}{2}\mu(\lambda_r^2 + \lambda_\theta^2 + \lambda_z^2 - 3) - \frac{\varepsilon}{2}(E_k E_k)^2 \quad , \tag{11}$$

where μ is the initial shear modulus, the index $k = r, \theta, z$ and where the Einstein summation convention is adopted. The incompressibility of the elastomer requires that μ = Y/3, where Y is its Young's modulus. Therefore, the in plane constitutive equations for the layer specialise to

$$D = -\frac{\partial W}{\partial E} = \varepsilon E, \tag{12}$$

$$\sigma_\theta - \sigma_r = \lambda_\theta \frac{\partial W}{\partial \lambda_\theta} - \lambda_r \frac{\partial W}{\partial \lambda_r} - DE =$$

$$= \mu(\lambda_\theta^2 - \lambda_\theta^{-2}\lambda_z^{-2}) - \varepsilon E^2, \quad (13)$$

where it is clearly seen that (11) admits the classical linear relationship (12) among electric displacement and electric field.

Eq. (8) can be employed to find σ_z at each point once σ_r has been computed.

In addition, the pressure difference $\sigma_r(r_e) - \sigma_r(r_i)$ becomes

$$\sigma_r(r_e) - \sigma_r(r_i) = \\ = \int_{r_i}^{r_e} \frac{1}{r}\left[\mu(\lambda_\theta^2 - \lambda_\theta^{-2}\lambda_z^{-2}) - \varepsilon\left(\frac{1}{r}\frac{V}{ln\frac{r_e}{r_i}}\right)^2\right] dr. \quad (14)$$

It is worth pointing out that, while a closed form of the integral in (14) can be obtained, this will not be given here.

C. Voltage-pressure relationship for the multilayer bandage

The voltage pressure relationship for the bandage in state $\mathcal{B}_V$ can be obtained by imposing continuity of the radial stresses at the interface between two generic concentric layers and the following boundary conditions:

$$\sigma_r(r_m) = -P_v, \;\; \sigma_r(r_{p2}) = 0. \quad (15)$$

A repeated use of (14), where V=0 in layers m, p_1 and p_2, yields

$$P_V = \int_{r_m}^{r_{p1}} \frac{\mu_m}{r}(\lambda_{\theta m}^2 - \lambda_{\theta m}^{-2}\lambda_{zm}^{-2})\, dr \\ + \int_{r_{p1}}^{r_{a1}} \frac{\mu_{p1}}{r}\left(\lambda_{\theta p1}^2 - \lambda_{\theta p1}^{-2}\lambda_{zp1}^{-2}\right) dr \\ + \int_{r_{a1}}^{r_{a1a2}} \frac{1}{r}\left[\mu_{a1}(\lambda_{\theta a1}^2 - \lambda_{\theta a1}^{-2}\lambda_{za1}^{-2}) - \varepsilon\left(\frac{1}{r}\frac{V}{ln\frac{r_{a1a2}}{r_{a1}}}\right)^2\right] dr \\ + \int_{r_{a1a2}}^{r_{a2}} \frac{1}{r}\left[\mu_{a2}(\lambda_{\theta a2}^2 - \lambda_{\theta a2}^{-2}\lambda_{za2}^{-2}) - \varepsilon\left(\frac{1}{r}\frac{V}{ln\frac{r_{a2}}{r_{a1a2}}}\right)^2\right] dr \\ + \int_{r_{a2}}^{r_{p2}} \frac{\mu_{p2}}{r}\left(\lambda_{\theta p2}^2 - \lambda_{\theta p2}^{-2}\lambda_{zp2}^{-2}\right) dr. \quad (16)$$

Assuming that the product between the pressure P_V and the air volume Vol inside the chamber only depends on the mechanical path (i.e. assuming that the temperature is constant) and assuming no air leakage from the chamber, the ideal gas law gives

$$P_V\, Vol = \text{constant}. \quad (17)$$

This condition allows for relating the inner radius of the rubber membrane r_m to the pressure P_v:

$$P_0\, \bar{r}_m^2 = P_V\, r_m^2. \quad (18)$$

By substituting (18) into (16), a relation between the air chamber pressure P_0 and the inner radius of the rubber membrane r_m is provided, once the driving voltage V is assigned:

$$\frac{\bar{r}_m^2}{r_m^2} P_0 = \int_{r_m}^{r_{p1}} \frac{\mu_m}{r}(\lambda_{\theta m}^2 - \lambda_{\theta m}^{-2}\lambda_{zm}^{-2})\, dr \\ + \int_{r_{p1}}^{r_{a1}} \frac{\mu_{p1}}{r}\left(\lambda_{\theta p1}^2 - \lambda_{\theta p1}^{-2}\lambda_{zp1}^{-2}\right) dr \\ + \int_{r_{a1}}^{r_{a1a2}} \frac{1}{r}\left[\mu_{a1}(\lambda_{\theta a1}^2 - \lambda_{\theta a1}^{-2}\lambda_{za1}^{-2}) - \varepsilon\left(\frac{1}{r}\frac{V}{ln\frac{r_{a1a2}}{r_{a1}}}\right)^2\right] dr \\ + \int_{r_{a1a2}}^{r_{a2}} \frac{1}{r}\left[\mu_{a2}(\lambda_{\theta a1a2}^2 - \lambda_{\theta a1a2}^{-2}\lambda_{za1a2}^{-2}) - \varepsilon\left(\frac{1}{r}\frac{V}{ln\frac{r_{a2}}{r_{a1a2}}}\right)^2\right] dr \\ + \int_{r_{a2}}^{r_{p2}} \frac{\mu_{p2}}{r}\left(\lambda_{\theta p2}^2 - \lambda_{\theta p2}^{-2}\lambda_{zp2}^{-2}\right) dr. \quad (19)$$

In order to calculate the contact pressure P_c it is important to define the pressure sustained by the rubber membrane of the air chamber P_m. Considering equation (19), for a certain value of the radius r_m the pressure P_m is given by the first term on the right-hand side of (16):

$$P_m = \int_{r_m}^{r_{p1}} \frac{\mu_m}{r}(\lambda_{\theta m}^2 - \lambda_{\theta m}^{-2}\lambda_{zm}^{-2})\, dr. \quad (20)$$

In the state $\mathcal{B}_V$, the contact pressure between the rubber membrane and the bandage is obtained by subtracting P_m from the air chamber pressure P_V:

$$P_c = P_V - P_m. \quad (21)$$

In order to quantify the contact pressure P_c it is necessary to know the shear moduli of the three materials (silicone, acrylic and rubber). For the passive layers, the quasi-static value 16 kPa experimentally determined by [24] was adopted for both the moduli μ_{p1} and μ_{p2}. For the acrylic elastomer, the value 73 kPa measured by [25] was used for both the moduli μ_{a1} and μ_{a2}. For the rubber membrane, the value 666 kPa reported in [26] was employed for the modulus μ_m.

VII. Model Validation: Comparison Between Experimental Data and Model Predictions

As a validation of the model, Fig. 6 presents a comparison between experimental data and model predictions.

The comparison shows that the model accuracy increases with the thickness of the passive layer. This outcome may be explained in terms of the constraining effect introduced by the stiffening sticks. Indeed, for the sample with 2 mm-thick passive layers the wooden sticks were closer to the electroactive layer, inducing local stress concentration and, so, limiting actuation. As in the model the presence of the stiffeners was ignored, these effects were not considered.

This might explain the discrepancy evident in Fig. 6a, especially at high voltages. Conversely, for the other extreme

case, i.e. for the 4 mm-thick passive layers, the stiffening sticks were significantly distant from the electroactive layer, such that stress concentration and expansion restraining were significantly reduced. This might justify the accurate match between experimental measurements and model predictions evident from Fig. 6c.

del prediction

Fig. 6. Dependence of the air chamber pressure P_V on the applied voltage V: comparison between experimental data and model-based predictions, for the three types of prototype bandages having different thickness D_p of their passive layers.

VIII. Model Predictions: Contact Pressure

The validated theoretical framework described above is particularly useful to compute the contact pressure P_c exchanged between the air chamber and the bandage in the 'Voltage ON' state. This is an important variable as, with reference to the intended application, it represents the pressure that would actually be exerted by the bandage on the surface of the user. Fig. 7 presents the estimates for the three prototype bandages, while Fig. 8 compares the contact pressure variation ΔP_c as a function of the applied voltage V for bandages having a passive layer's thickness from 0 to 4 mm and a length of the inner circumference of the passive layer p_1 equal to L=260 mm.

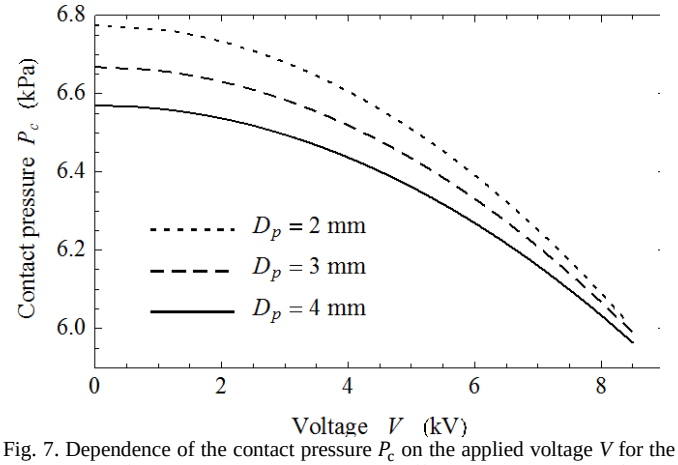

Fig. 7. Dependence of the contact pressure P_c on the applied voltage V for the three types of prototype bandages having different thickness D_p of their passive layers.

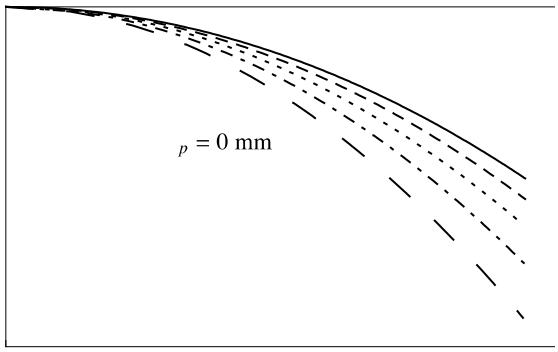

Fig. 8. Variation of the contact pressure between the air chamber and the bandage, as estimated from the model for bandages having a different thickness D_p of the passive layers.

Fig. 7 shows the contact pressure-voltage curves for the three prototypes. The curves intersect close to the experimental breakdown limit. For D_p=2, 3 and 4 mm the estimated initial contact pressure was 6.78, 6.67 and 6.57 kPa, respectively, and upon actuation at 8 kV the pressure respectively dropped to 6.09, 6.06 and 6.03 kPa, corresponding to a reduction of 10.2%, 9.15% and 8.2%. These estimates indicate that the contact pressure change was highest for the sample featuring the thinnest passive layers.

The fact that the model predicts a higher performance for a lower thickness of the passive layers is also evident from Fig. 8, which plots the pressure variation also for values of thickness not tested experimentally.

So, according to the model, the highest performance would be achieved without any passive layer. This outcome is due to the fact that the presence of the stiffeners was neglected by the simplified model. Therefore, further developments of the

model are needed in order to take in account the effect of the stiffeners. By taking into account the stiffeners, it is reasonable to expect an optimum value of the passive layer thickness, which should maximise the contact pressure variation.

IX. Future Developments

A. Improvement of the electromechanical properties

In order to study the influence of the number of electroactive layers on the actuator's ability to vary the contact pressure, the simulations shown in Fig. 9 were performed. They refer to bandages having D_p=2 mm and an increasing number of active layers with properties identical to those considered above. The simulations show that the higher the number of active layers, the larger is the contact pressure variation, although it tends to saturate.

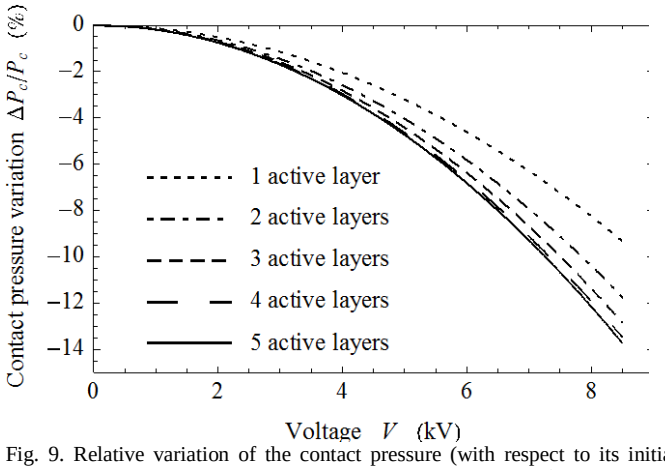

Fig. 9. Relative variation of the contact pressure (with respect to its initial value) between the air chamber and the bandage, as estimated from the model for five types of prototype bandages having an increasing number of active layers and a constant thickness of the passive layers D_p= 2 mm.

Fig. 10 visualises the saturation trend of the contact pressure variation $\Delta P_c/P_c$ for bandages having up to 10 active layers and with V=8 kV.

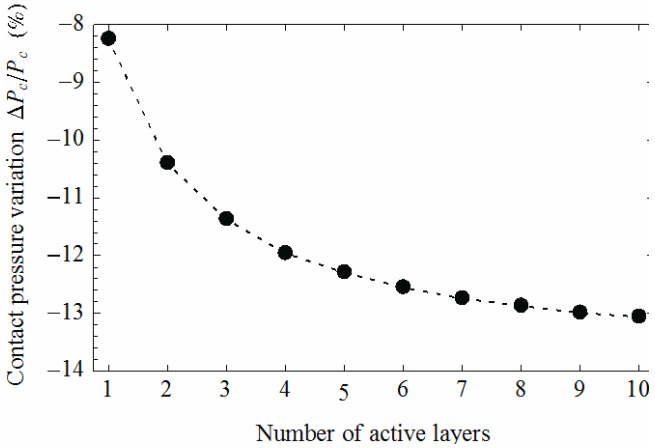

Fig. 10. Relative variation of the contact pressure (with respect to its initial value) at V=8 kV between the air chamber and the bandage, as estimated from the model for ten samples of prototype bandage having an increasing number of active layers and a constant thickness of the passive layers D_p= 2 mm.

This outcome is plausible as it is consistent with the intuitive view that, as the total number of layers increases, any constraint at the surfaces of the cylindrical stack tends to have a vanishing influence on the 'central' layers that are 'sufficiently distant' from the ends. Moreover, as the total number of layers increases, the number of the 'central' layers unaffected by the constraint increases, such that the unaffected portion of stack is larger. So, as the stack grows up, it gets closer to an ideal infinitely thick structure, whose generated force is not affected by any constraint at the two ends and by the number of layers: it would generate the same force as that generated by a single ideal unloaded layer. Knowing that such a saturation effect exists is useful for the design of multi-layered electroactive bandages.

B. Improvement of the model

To improve the accuracy of the model, the presence of the stiffening sticks should be taken into account. Such a detailed modelling was beyond the aims of this first investigation and should be tackled in future studies.

C. High-voltage driving: viability and challenges

These prototype bandages required driving voltages of several kilovolts. In terms of electrical safety, dealing with such high voltages is clearly not desirable. However, this drawback is mitigated not only by the use of insulating layers, but, especially, by the fact that there's no need for a high driving current (and, so, power). Indeed, electrically the bandage is a capacitive load, which allows for using low-power, electrically safe sources.

The low power requirement favours also the technical viability of high voltage driving. Indeed, high-voltage multipliers with low-power and compact size (volume of the order of 1 cm^3 or less) are commercially available such as those produced by EMCO High Voltage [27]. This allows for implementations of battery-powered portable and compact systems.

Nevertheless, the need for high-voltage circuitry introduces a significant limitation in terms of costs. This drawback, which is characteristic for the whole field of the DE transducers today, is focusing efforts to produce films that can be driven at lower voltages. Besides fundamental attempts to synthesize new elastomers with higher dielectric constant [28], [29], the most readily achievable solution in the short term is represented by thin-film processing of conventional materials [17]. Indeed, several groups have already demonstrated DE transducers with voltages reduced to a few hundred volts [30], thus anticipating that in the near future the DE technology will likely adopt the standard and cheaper circuitry used today for piezoelectric drives.

X. Conclusions

We presented here a multilayer active bandage made of dielectric elastomer actuators. This study showed the following main evidences.

First, the passive layers coating the bandage have a function that goes beyond those of electrical protection and mechanical impedance matching. Indeed, as shown by both the experiments and analytical model, they play a key role for an

effective transmission of actuation from the active layers to the load.

The second evidence is that by adopting the multilayer design reported above and different constitutive materials, it was possible to achieve a higher contact pressure drop as compared to previous studies. Indeed, the best performing active bandage prototype reported in [10] allowed for achieving an initial contact pressure of 2.87 kPa and a drop to 2.73 kPa, corresponding to a 5.2% decrease, for a voltage of 11.3 kV; in comparison, the active bandage prototypes presented here allowed for contact pressures ranging from 6.57 kPa to 6.78 kPa and, respectively, pressure drops from 8.2% to 10.2%, for a voltage of 8.5 kV.

The third evidence is that, according to the new design, the existence of an optimum value of the passive layer thickness is expected. However, such value could not be precisely identified here, owing to the need for advanced models able to capture the complexity of the constraints introduced by the stiffening elements.

The fourth evidence is that, for a given passive layer's thickness, the variation of contact pressure increases with the number of active layers, with a saturation trend.

These outcomes, together with the theoretical framework specifically developed for the case of prestretched multiple layers, are expected to serve as help for future improvements of the design, implementation and manufacturing process of prestretched multi-layer electroactive bandages.

APPENDIX

The general constitutive equations for an electroactive, incompressible, isotropic dielectric elastomer expressed in terms of principal stretches λ_i, electric field E_i and electric displacement field D_i (i=1,2,3) are obtained below. In the following, in order to maintain the Einstein convention implying summation over an index repeated twice, for generic quantities A_i and B_i (i=1,2,3) it is useful to introduce the notations $[A/B]_i$ and $[AB]_i$ which correspond to A_i/B_i and $A_i B_i$, respectively.

Due to the large strains accompanying the deformation of DE materials, constitutive equations are usually defined in terms of nominal quantities, such as principal components of nominal total stress S_i, nominal electric field $E^0{}_i$ and nominal electric displacement $D^0{}_i$, via a free energy $H(\lambda_i, E^0{}_i)$ as [31]:

$$S_i=\frac{\partial H}{\partial \lambda_i}+q\frac{1}{\lambda_i}, \tag{A1}$$

$$\frac{\partial H}{\partial E_i^0}=-D_i^0, \tag{A2}$$

where q is a pressure term defined by boundary conditions.

These forms are implied by the expression of the change $\dot{H}$ of H brought about by independent changes $\dot{\lambda}_i$ and $\dot{E}_i^0$

$$\dot{H}\ =S_i\dot{\lambda}_i+q\frac{\dot{\lambda}_i}{\lambda_i}-D_i^0\dot{E}_i^0. \tag{A3}$$

As shown by isotropic finite-strain electro-mechanics, along principal axes $E^0{}_i=[\lambda E]_i$, $D^0{}_i=[D/\lambda]_i$ and $S_i=[\sigma/\lambda]_i$, so that introducing the function $W(\lambda_i, E_i)= H(\lambda_i, [\lambda E]_i)$, it turns out that eq. (A3) is equivalent to

$$\frac{\partial W}{\partial \lambda_i}\dot{\lambda}_i+\frac{\partial W}{\partial E_i}\dot{E}_i=\left[\frac{\sigma}{\lambda}\right]_i\dot{\lambda}_i+q\frac{\dot{\lambda}_i}{\lambda_i}-\left[\frac{D}{\lambda}\right]_i\left\{\left[\dot{\lambda}E\right]_i+\left[\lambda\dot{E}\right]_i\right\}, \tag{A4}$$

which corresponds to

$$\frac{\partial W}{\partial E_i}=-D_i \tag{A5}$$

$$\frac{\partial W}{\partial \lambda_i}=\left[\frac{\sigma}{\lambda}\right]_i+q\frac{1}{\lambda_i}-\left[\frac{D}{\lambda}E\right]_i. \tag{A6}$$

In particular, (A6) can be rewritten as

$$\sigma_i=\lambda_i\frac{\partial W}{\partial \lambda_i}-q+D_iE_i \text{ (no sum on index } i\text{)}, \tag{A7}$$

which is employed in section VI.B.

ACKNOWLEDGMENTS

The authors gratefully acknowledge funding from the European Community's 7th Framework Programme ([FP7/2007-2013]) via the project **"**STAMAS - Smart technology for artificial muscle applications in space" (grant agreement n° 312815).

REFERENCES

[1] R. T. Eberhardt and J. D. Raffetto, "Chronic venous insufficiency," *Circulation*, vol. 111, no. 18. pp. 2398–2409, 2005.

[2] M. Brignole and D. G. Benditt, "Pathophysiology of Syncope," in *Syncope*, London: Springer London, pp. 15–25, 2011.

[3] T. Lewis, "A Lecture on Vasovagal Syncope and The Carotid Sinus Mechanism," *BMJ*, vol. 1, no. 3723, pp. 873–876, 1932.

[4] A. H. Chen, S. G. Frangos, S. Kilaru, and B. E. Sumpio, "Intermittent Pneumatic Compression Devices – Physiological Mechanisms of Action," *Eur. J. Vasc. Endovasc. Surg.*, vol. 21, no. 5, pp. 383–392, 2001.

[5] J. J. Bergan, G. W. Schmid-Schönbein, P. D. C. Smith, A. N. Nicolaides, M. R. Boisseau, and B. Eklof, "Chronic Venous Disease," *N. Engl. J. Med.*, vol. 355, no. 5, pp. 488–498, 2006.

[6] H. Partsch, M. Clark, G. Mosti, E. Steinlechner, J. Schuren, M. Abel, J.-P. Benigni, P. Coleridge-Smith, A. Cornu-Thénard, M. Flour, J. Hutchinson, J. Gamble, K. Issberner, M. Juenger, C. Moffatt, H. A. M. Neumann, E. Rabe, J. F. Uhl, and S. Zimmet, "Classification of Compression Bandages: Practical Aspects," *Dermatologic Surg.*, vol. 34, no. 5, pp. 600–609, 2008.

[7] N. H. Hills, J. J. Pflug, K. Jeyasingh, L. Boardman, and J. S. Calnan, "Prevention of Deep Vein Thrombosis by Intermittent Pneumatic Compression of Calf," *BMJ*, vol. 1, no. 5793, pp. 131–135, 1972.

[8] A. G. G. Turpie, "Prevention of Deep Vein Thrombosis in Potential Neurosurgical Patients," *Arch. Intern. Med.*, vol. 149, no. 3, p. 679, 1989.

[9] F. Chen, M. Y. Wang, J. Zhu and Y. F. Zhang, "Interactions between dielectric elastomer actuators and soft bodies," *Soft Robotics*, vol. 3, no. 4, pp. 161-169, 2016.

[10] S. Pourazadi, S. Ahmadi, and C. Menon, "Towards the development of active compression bandages using dielectric elastomer actuators," *Smart Mater. Struct.*, vol. 23, no. 6, p. 65007, 2014.

[11] S. Pourazadi, S. Ahmadi, and C. Menon, "On the design of a DEA-based device to pot entially assist lower leg disorders: an analytical and FEM investigation accounting for nonlinearities of the leg and device deformations," *Biomed. Eng. Online*, vol. 14, no. 1, p. 103, 2015.
[12] F. Carpi and E. Smela, Editors, *Biomedical Applications of Electroactive Polymer Actuators*, Chichester: Wiley, 2009.
[13] F. Carpi, Editor, *Electromechanically Active Polymers: a Concise Reference*, Zurich: Springer, 2016.
[14] R. Pelrine, R. Kornbluh, Q. Pei, J. Joseph, "High-speed electrically actuated elastomers with strain greater than 100%," *Science*,vol. 287, pp. 836–9, 2000.
[15] F. Carpi, D. De Rossi, R. Kornbluh, R. Pelrine and P. Sommer-Larsen, Editors, *Dielectric Elastomers as Electromechanical Transducers. Fundamentals, Materials, Devices, Models and Applications of an Emerging Electroactive Polymer Technology*, Oxford: Elsevier, 2008.
[16] P. Brochu and Q. Pei, "Advances in Dielectric Elastomers for Actuators and Artificial Muscles," *Macromol. Rapid Commun.*, vol. 31, no. 1, pp. 10–36, 2010.
[17] F. Carpi, S. Bauer, and D. De Rossi, "Stretching Dielectric Elastomer Performance," *Science*, vol. 330, , pp. 1759-1761, 2010.
[18] T. Lu, J. Huang, C. Jordi, G. Kovacs, R. Huang, D. R. Clarke, and Z. Suo, "Dielectric elastomer actuators under equal-biaxial forces, uniaxial forces, and uniaxial constraint of stiff fibers," *Soft Matter*, vol. 8, no. 22, pp. 6167–6173, 2012.
[19] R. Liu, Y. L. Kwok, Y. Li, T. T. H. Lao, X. Zhang, and X. Q. Dai, "Objective Evaluation of Skin Pressure Distribution of Graduated Elastic Compression Stockings," *Dermatologic Surg.*, vol. 31, no. 6, pp. 615–624, 2006.
[20] S. J. A. Koh, T. Li, J. Zhou, X. Zhao, W. Hong, J. Zhu, and Z. Suo, "Mechanisms of large actuation strain in dielectric elastomers," *J. Polym. Sci. Part B Polym. Phys.*, vol. 49, no. 7, pp. 504–515, 2011.
[21] S. Roccabianca, M. Gei, and D. Bigoni, "Plane strain bifurcations of elastic layered structures subject to finite bending: theory versus experiments," *IMA J. Appl. Math.*, vol. 75, no. 4, pp. 525–548, Aug. 2010.
[22] F. Carpi and D. De Rossi, "Dielectric elastomer cylindrical actuators: electromechanical modelling and experimental evaluation," *Mater. Sci. Eng. C*, vol. 24, no. 4, pp. 555–562, 2004.
[23] J. Zhu, H. Stoyanov, G. Kofod, and Z. Suo, "Large deformation and electromechanical instability of a dielectric elastomer tube actuator," *J. Appl. Phys.*, vol. 108, no. 7, p. 74113, 2010.
[24] F. Galantini, F. Carpi, and G. Gallone, "Effects of plasticization of a soft silicone for dielectric elastomer actuation," *Smart Mater. Struct.*, vol. 22, no. 10, p. 104020, 2013.
[25] M. Bozlar, C. Punckt, S. Korkut, J. Zhu, C. Chiang Foo, Z. Suo, and I. A. Aksay, "Dielectric elastomer actuators with elastomeric electrodes," *Appl. Phys. Lett.*, vol. 101, no. 9, p. 91907, 2012.
[26] M. E. Raghunandan, J. S. Sharma, and B. Pradhan, "A review on the effect of rubber membrane in triaxial tests," *Arab. J. Geosci.*, vol. 8, no. 5, pp. 3195–3206, 2015.
[27] "Emco, high voltage corporation." [Online]. Available: http://www.emcohighvoltage.com.
[28] F. B. Madsen, A. E. Daugaard, S. Hvilsted, and A. L. Skov, "The Current State of Silicone-Based Dielectric Elastomer Transducers," *Macromol. Rapid Commun.*, vol. 37, no. 5, pp. 378–413, 2016.
[29] S. J. Dünki, Y. S. Ko, F. A. Nüesch, and D. M. Opris, "Self-Repairable, High Permittivity Dielectric Elastomers with Large Actuation Strains at Low Electric Fields," *Adv. Funct. Mater.*, vol. 25, no. 16, pp. 2467–2475, 2015.
[30] A. Poulin, S. Rosset, and H. R. Shea, "Printing low-voltage dielectric elastomer actuators," *Appl. Phys. Lett.*, vol. 107, no. 24, p. 244104, 2015.
[31] A. Dorfmann and R. W. Ogden, "Nonlinear electroelasticity," *Acta Mech.*, vol. 174, no. 3–4, pp. 167–183, 2005.

Luigi Calabrese was born in Chiusi, Siena, Italy in 1986. He received the Laurea degree in Civil Engineering from the University of Perugia, Perugia, Italy in 2011 and a Master degree in Structural Engineering from the University of Trento, Trento, Italy in 2015. He is currently perusing a Ph.D. degree in Modeling and Simulation within the Doctoral Programme in Civil, Environmental and Mechanical Engineering at University of Trento. Since 2015 he has been with the Interdepartmental Research Center "E. Piaggio," School of Engineering, University of Pisa, where he is currently a research fellow. His research interests focus on the development of electroactive-polymer-based mechatronic devices. Since 2014 he is member of the EuroEAP Society where he volunteers as president of the Dissemination & Outreach Committee.

Gabriele Frediani from 2006 to 2012 worked as a research fellow at the Interdepartmental Research Centre "E. Piaggio", School of Engineering, University of Pisa, performing research activities in the framework of several European research projects (Such as CEEDS and Viactors) and contracts (such as ESA EAP Actuators and L'Oreal). In 2013 he started a PhD studentship at Queen Mary University of London an in 2017 he was awarded the title of PhD in Medical engineering. He is currently a research fellow at the University of Florence, Department of Industrial Engineering. His activities are focused on the design, manufacturing and testing of new tactile devices based on DEA, although a number of other different areas of application have been explored as well, such as systems for the biomedical and bioinspired fields.

Massimiliano Gei is Professor of Solid Mechanics and Structures at the School of Engineering of Cardiff University, UK. After the degree in Civil Engineering awarded in 1997 by the University of Bologna, he received in 2001 the Ph.D. in Materials and Structural Engineering from the University of Trento. Post-doc at the University of Modena and Reggio Emilia between 2001 and 2003, from 2005 to 2015 he was with the University of Trento as Assistant Professor (2005-2011) and Associate Professor

(2011-2015). At Cardiff University he is currently leading the Applied and Computational Mechanics group. His research activities are in the fields of soft smart structures, composite materials and mechanical metamaterials. He has co-authored more than 40 papers on international journals.

Danilo De Rossi was awarded the title of Doctor in Chemical Engineering at the University of Genoa in 1976. From 1976 to 1981 he was researcher of the Institute of Clinical Physiology of C.N.R. He had appointments for teaching and research in France, USA, Brazil, Japan and Australia. Since 1982 he has been working in the School of Engineering of the University of Pisa, where he is presently Full Professor of Bioengineering. His scientific activities are related to the design of sensors and actuators for bioengineering and robotics and to the study and development of wearable systems for telemonitoring and telerehabilitation. He received the Young Investigator Forum Award from Biomedical Engineering Society (UK) in 1980 and from the American Society for Artificial Internal Organs in 1985. In 2012 he was awarded of the Order of the Cherubino from the University of Pisa for institutional and scientific values. He is author of over 300 peer-reviewed papers on international science journals and peer reviewed proceedings, co-inventor of 14 patents and co-author of 10 books.

Federico Carpi is an Associate Professor in Biomedical Engineering at the University of Florence, Department of Industrial Engineering, Florence, Italy. He received from the University of Pisa the Laurea degree in Electronic Engineering, the Ph.D. degree in Bioengineering and a second Laurea degree in Biomedical Engineering. From 2005 to 2012 he has been a post-Doc researcher at the University of Pisa and from 2012 to 2016 an Associate Professor in Biomedical Engineering and Biomaterials at Queen Mary University of London. From 2010 to 2014 he has been the Chair of the 'European Scientific Network for Artificial Muscles (ESNAM)', focused on transducers and artificial muscles based on electroactive polymers and from 2013 to 2017 he has served as the first President of the ‘EuroEAP Society’ (www.euroeap.eu). His publications include some 70 articles in international journals, 3 edited books and several contributions to books and conferences.